

This is a self-archived version of an original article. This version may differ from the original in pagination and typographic details.

Author(s): Papadakis, Philippos; Liimatainen, Jarkko; Sarén, Jan; Moore, Iain; Eronen, Tommi; Partanen, Jari; Pohjalainen, Ilkka; Rinta-Antila, Sami; Tuunanen, Juha; Uusitalo, Juha

Title: The MARA-LEB ion transport system

Year: 2020

Version: Accepted version (Final draft)

Copyright: © 2019 Elsevier B.V.

Rights: CC BY-NC-ND 4.0

Rights url: <https://creativecommons.org/licenses/by-nc-nd/4.0/>

Please cite the original version:

Papadakis, P., Liimatainen, J., Sarén, J., Moore, I., Eronen, T., Partanen, J., Pohjalainen, I., Rinta-Antila, S., Tuunanen, J., & Uusitalo, J. (2020). The MARA-LEB ion transport system. *Nuclear Instruments and Methods in Physics Research. Section B: Beam Interactions with Materials and Atoms*, 463, 268-289. <https://doi.org/10.1016/j.nimb.2019.05.007>

The MARA-LEB ion transport system

P. Papadakis^{a,b}, J. Liimatainen^a, J. Sarén^a, I.D. Moore^a, T. Eronen^a, J. Partanen^a, I. Pohjalainen^a, S. Rinta-Antila^a, J. Tuunanen^a, J. Uusitalo^a

^aUniversity of Jyväskylä, Department of Physics, P.O. Box 35, FI-40014 University of Jyväskylä, Finland

^bDepartment of Physics, Oliver Lodge Laboratory, University of Liverpool, Liverpool, L69 7ZE, United Kingdom

Abstract

A low-energy branch is under development for the MARA vacuum-mode recoil separator at the Accelerator Laboratory of the University of Jyväskylä. This development will allow for the study of proton-rich nuclei through laser ionisation spectroscopy and mass measurements. After stopping and extraction from a buffer gas cell, the ions of interest will be accelerated and transported to dedicated experimental setups by an ion transport system consisting of several focusing, accelerating and mass-separating elements. This article presents the current design and simulations for the ion transport.

Keywords: MARA, ion guide, ion optics, low-energy branch

1. Introduction

The MARA Low-Energy Branch (MARA-LEB) [1, 2] will focus on the experimental investigation of exotic nuclei close to the proton drip line. It will be employed at the focal plane of the MARA [3, 4] vacuum-mode recoil separator at the Accelerator Laboratory of the University of Jyväskylä, Finland (JYFL). The ions of interest will be produced in fusion-evaporation reactions and after mass separation through MARA they will be stopped and thermalised in a small-volume buffer gas cell at the focal plane of the separator. The ions will be neutralised using argon buffer gas in order to subsequently perform laser ionisation and spectroscopy studies. For mass measurement experiments, helium buffer gas will be used, providing faster extraction from the gas cell.

The primary area of interest for MARA-LEB is in the region of the heaviest known self-conjugate nuclei. Key nuclei close to ^{80}Zr , ^{94}Ag and ^{100}Sn provide a fertile testing ground for nuclear models and their predictive powers (see for example [6]). In addition, several nuclei in this region largely influence the nucleosynthesis models and are significant in modeling and understanding the astrophysical rapid proton capture (rp) process [7, 8].

MARA is ideal for pursuing studies in the aforementioned regions of interest. The mass selectivity it provides combined with a mass slit system for suppressing ions with unwanted mass per charge ratio will be crucial for the investigation of exotic nuclei close to the $N=Z$ line. The first experimental campaign of MARA was highly successful with five new isotopes identified. During the campaign the transmission (30-50%) and mass resolving capabilities of the separator were found to be in agreement with ion-optical calculations [4].

The gas cell design for MARA-LEB is similar to that for S3-LEB, GANIL [5], matched to accept two charge states from the MARA recoil separator. It has been refined using detailed gas flow simulations and incorporates several features that aim to optimise its performance. These include separate volumes for the stopping and re-ionisation of recoils, use of ion collector-electrodes for suppressing non-neutralised recoils from exiting the gas cell and structures for reducing gas turbulence in the gas cell volume. These features increase selectivity and reduce losses within the gas cell caused by collisions with the walls. Further details on MARA-LEB as well as the scientific motivation for the facility can be found in [1, 2]. In this article we present the design and simulations for the ion transport to the focal plane of the MARA-LEB facility.

2. Ion-optical transport system

The ion-optical system which will transport the ions of interest from the exit of the gas cell to the experimental stations can be separated into two parts: (a) the primary ion guides and acceleration optics and (b) the ion transfer line.

2.1. Primary ion guides and acceleration optics

Ions exiting the gas cell will be focused and accelerated to 30 kV to increase transmission efficiency to the experimental stations. The ambient pressure in the gas cell volume will be significantly higher than the pressure required for the operation of the accelerating electrodes. Therefore, a two-stage differential pumping system will be used to incrementally reduce the background pressure to the order of 10^{-6} - 10^{-7} mbar.

The ions will be transported through the three differential pumping regions by the ion guides presented in Figure 1c. In the first region, a 90°-bent radio-frequency quadrupole (RFQ) ion guide will direct the ions towards the second chamber. The

Email address: philippos.papadakis@liverpool.ac.uk (P. Papadakis)

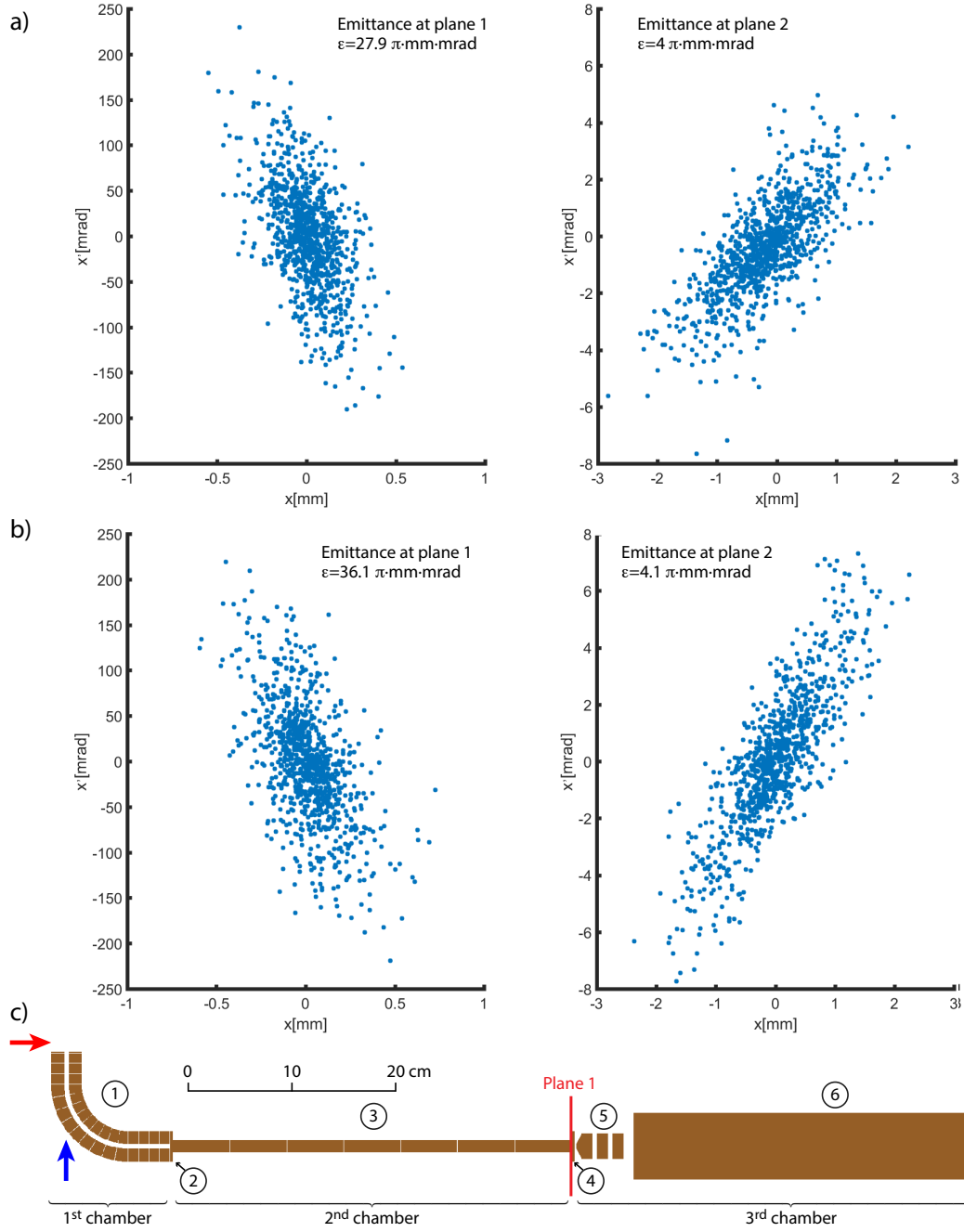


Figure 1: a): Simulated emittance plots at plane 1 (left) and at plane 2 (right) for 1000 $^{94}\text{Ag}^+$ ions. Helium at 500 mbar pressure was used as the buffer gas and the exit hole with a diameter of 0.5 mm allowed for a free expanding jet. The emittances in the y direction are almost identical. b) Same as a) but using 500 mbar argon as the buffer gas. c) Current design of the primary ion guides and acceleration optics for MARA-LEB. The vacuum chamber in which each component will be positioned is marked at the bottom of the figure. (1) is the 90°-bent RFQ, (2) and (4) the pumping apertures, (3) is the straight segmented RFQ, (5) the three acceleration electrodes and (6) the ground electrode. The red and blue arrows indicate the direction of the transverse and longitudinal lasers for in-gas-jet laser ionisation, respectively.

90° bend was introduced for the following reasons: (a) to provide access to the longitudinal laser beam which will be used for in-gas-jet laser ionisation without having to pass the laser through the pumping apertures. Therefore, the pumping aperture diameter can be made smaller to reduce the gas throughput between chambers; (b) to place the aperture to the second chamber on a different geometrical axis to the gas jet thus reducing the amount of gas particles transported by the jet into

the chamber; (c) due to space restrictions. A 2.5-mm radius pumping aperture separating the two volumes will be placed on the same potential as the last element of the bent RFQ to ensure continuity in the electric field. A straight, segmented RFQ will confine and transport the ions to the third vacuum region where they will be accelerated stepwise to the final potential of 30 kV.

The first conical accelerating electrode will be followed by two cylindrical electrodes. These three can either be used as

an Einzel lens or for changing the potential in smaller steps. A ground electrode will provide the final acceleration step. In MARA-LEB the gas cell will be placed at 30 kV while the ion transport line and experimental setups will be at ground potential.

Simulations of the ion guides were performed using the SIMION software package [9]. Results from these simulations are presented in Figure 1. The figure shows the emittance plots recorded after the straight RFQ (plane 1) and the ground electrode (plane 2) for 1000 $^{94}\text{Ag}^+$ ions. The ions were produced in a 60° cone which emulates the focusing of a free-expanding gas jet produced by a round orifice [10]. A similar angle of ion emission was chosen during the development of the radio-frequency sextupole ion guide for the IGISOL facility [11]. Helium gas at 500 mbar pressure was used as buffer gas for the simulations presented in Figure 1a, while argon gas at the same pressure for the results in Figure 1b. The voltages applied at various positions in the simulation are listed in Table 1.

Table 1: Voltages used at various positions in the simulations presented in Figure 1. All voltages were the same for helium and argon except for the RF voltage applied to the 90° -bent RFQ. The value for argon is given in brackets. The voltage step between the electrodes of the RFQs was 1 V and the frequency of the RF component was 1 MHz.

Position	Voltage [V]
Gas cell	30000
90° -bent RFQ, first electrode	29980
90° -bent RFQ, last electrode	29963
90° -bent RFQ RF voltage	175 [225]
1 st pumping aperture	29963
Straight RFQ, first electrode	29962
Straight RFQ, last electrode	29956
Straight RFQ RF voltage	40
2 nd pumping aperture	29956
Einzel lens, first and last segment	15000
Einzel lens, middle segment	30000
Ground electrode	0

The SIMION code by default calculates ion trajectories in vacuum. Therefore, ion-gas collision models had to be introduced in the simulation to realistically account for the interaction of ions with residual gas. A hard sphere model was used [12] for pressures lower than 8 mbar. This model becomes impractical with increasing pressure due to long computation times as a result of the high number of ion-gas collisions. Therefore, for pressures higher than 8 mbar a statistical diffusion model was used. This model uses collision statistics to significantly reduce computation times and has been experimentally validated in the pressure region from 8 to 850 mbar [13].

The gas pressure, temperature and velocity at various positions after the exit hole were calculated based on the Mach number to realistically model the free expanding jet, since these have an effect on ion-gas collision calculations. Initially the Mach disk location and the local Mach number at each position (M_{loc}) were calculated using the equations in [14]. For argon gas the terminal Mach number was determined as $M_T=30$ and

M_{loc} was allowed to increase until this value was reached. In the case of helium the same approach was not possible due to complications introduced by quantum effects [15]. Thus the Mach number was increased as a function of position until the location of the Mach disk where it reached the value $M_{loc}=21$. After the Mach disk location the gas velocity was decreased linearly in both cases.

As an alternative to the use of free expanding jets, de Laval nozzles [16] specified for different Mach numbers can be used to produce collimated jets suitable for high-resolution in-gas-jet laser ionisation spectroscopy. Simulations of free expanding and collimated gas jets have recently been performed and were found to reproduce experimental results with high accuracy [17]. Simulations for the design of de Laval nozzles for use with MARA-LEB will be performed in collaboration with the authors of [17].

In the simulations presented in Figure 1, the ion-beam profile is found to be cylindrical across the ion guides. The emittance in the y direction is almost identical to that for the x direction and so has been omitted from the figure. The mean energy of the ions at plane 1 is 369 eV with a spread of 8 eV. The higher energy compared to the values anticipated from Table 1 is caused by penetration of the accelerating potential in the straight-RFQ region. At plane 2 the mean energy is 29.95 keV with a spread of 0.03 keV. The total transmission efficiency from the gas cell exit hole until plane 2 is 97% with helium buffer gas and 96% with argon.

2.2. Ion transfer line

The accelerated ions will be mass separated and focused to an electrostatic switchyard at the focal point of the mass separator using a series of ion-optical elements, before delivery to the experimental stations. A quadrupole doublet will defocus the beam in the vertical plane to disperse the ion trajectories within a dipole mass separator. This will enhance the mass resolving power of the separator. The dipole magnet has a 1.0 m bending radius, pole iron gap of 50 mm and a maximum field of 0.5 T. In addition to mass separation the dipole magnet will divert the ion beam into a vertical beam line to guide the ions towards the second floor of the accelerator laboratory where the experimental stations will be housed. An electrostatic 90° deflector at the top of the beam line will direct the beam from the vertical line back to the horizontal plane on the second floor. The electrostatic quadrupoles will be manufactured in-house and their design is based on similar devices built and used in the laboratory.

Between the magnetic dipole and the deflector there is a focal point which is to be used for further mass selection. The mass resolving power at this point is estimated to be in the region of 350 based on the emittances yielded by the SIMION simulations of the primary ion guides and acceleration optics described earlier. This focal point will be equipped with a mass slit system which can be used to suppress unwanted isobars. The design of this system is based on the one in use at MARA [3]. The layout of the transfer line and one possible ion-optical solution are shown in Figure 2. The figure illustrates three ion trajectories with inclination angles -10, 0 and 10 mrad in the

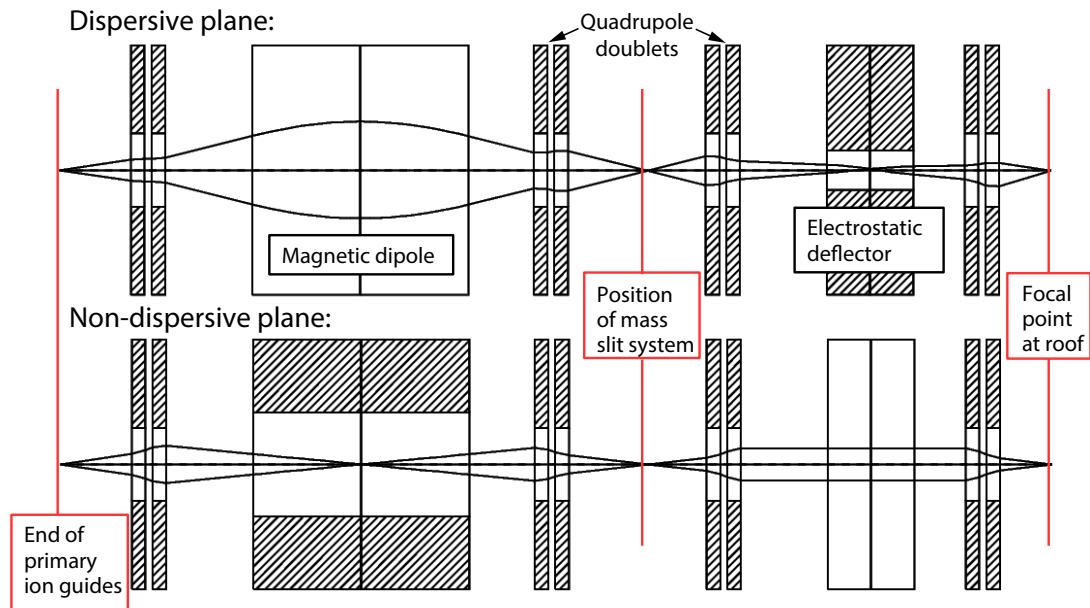


Figure 2: Ion-optical solution of the transfer line from the accelerating electrodes to the focal point of the mass separator on the second floor of the laboratory. An electrostatic switchyard will be placed at this point to divert the beam to the various experimental setups. Three trajectories are shown with inclination angles of -10 , 0 and 10 mrad for both the dispersive and non-dispersive planes. The dipole magnet and electrostatic deflector will bend the ions by 90° to divert them towards the experimental stations. Ions will be focused using electrostatic quadrupole doublets. Shaded areas in the figure denote the presence of solid material.

dispersive and non-dispersive planes. Calculations were performed using the computer code GICOSY [18]. More precise simulations will be run after all the constraints regarding the available space are finalised.

Acknowledgments

The MARA-LEB buffer gas cell was developed in collaboration with KU Leuven. The research leading to these results has received funding from the People Programme (Marie Curie Actions) of the European Union's Seventh Framework Programme (FP7/2007-2013) under REA grant agreement n° 626518. Funding from the Academy of Finland was received through the FIRI research infrastructure programme grant agreement number n° 293408 and the Finnish Centre of Excellence Programme 2012-2017 (Nuclear and Accelerator Based Physics).

[1] P. Papadakis et al., *Hyperfine Interactions* 237 (2016) 152.
 [2] P. Papadakis et al., *AIP Conference Proceedings* 2011 (2018) 070013.
 [3] J. Sarén, PhD Thesis, University of Jyväskylä (2011).
 [4] J. Uusitalo, J. Sarén, J. Partanen, J. Hilton, *Acta Phys. Pol. B* 50 (2019) 319.
 [5] Yu. Kudryavtsev et al., *Nucl. Instrum. Meth. B* 376, (2016) 345.
 [6] T. Faestermann, M. Gorska, H. Grawe, *Prog. in Part. and Nucl. Phys.* 69 (2013) 85.
 [7] R.K. Wallace and S.E. Woosley, *Astrophys. J. Suppl. Ser.* 45, (1981) 389.
 [8] H. Schatz and W.-J. Ong *The Astrophysical Journal* 844 (2017) 139.
 [9] S.I.S Inc., Simion 8.1, 1027 Old York Rd., Ringoes, NJ, USA.
 [10] Yu. Kudryavtsev et al., *Nucl. Instr. Methods B* 297 (2013) 7.
 [11] P. Karvonen et al., *Nucl. Instr. Methods B* 266 (2008) 4794.
 [12] A.D. Appelhans and D.A. Dahl, *Int. J. of Mass Spec.* 216 (2002) 269.
 [13] A.D. Appelhans and D.A. Dahl, *Int. J. of Mass Spec.* 244 (2005) 1.
 [14] H. Ashkenas, F.S. Sherman, *The structure and utilization of supersonic free jets in low density wind tunnels*, in: *Rarefied Gas Dynamics*, Academic Press, New York, 1966, p. 94.

[15] J.P. Toennies and K. Winkelmann, *J. Chem. Phys.* 66 (1977) 3965.
 [16] G. Dupeyrat, J.B. Marquette and B.R. Rowe, *Physics of Fluids* 28, 1273 (1985).
 [17] A. Zadornaya et al., *Phys. Rev. X* 8 (2018) 041008.
 [18] M. Berz, B. Hartmann, K. Lindemann, A. Magel, H. Weick, <https://web-docs.gsi.de/~weick/gicosy/>